ELSEVIER

Journal of Power Sources 86 (2000) 202–213

JOURNAL OF POWER SOURCES

www.elsevier.com/locate/jpowsour

Conceptual design and modeling of a fuel cell scooter for urban Asia

Bruce Lin *

Center for Energy and Environmental Studies, Princeton University, Princeton, NJ 08544 USA

Accepted 12 November 1999

Abstract

Air pollution is of serious concern in many Asian countries, especially in densely populated cities with many highly polluting two-stroke engine vehicles like scooters. Four-stroke engines and electric battery-powered scooters are often proposed as alternatives, but a fuel cell scooter would be superior by offering both zero tailpipe emissions and combustion-scooter class range (200 km) without lengthy battery recharging times. This advanced scooter concept is explored here. A conceptual polymer electrolyte membrane fuel cell scooter design with compact metal hydride hydrogen storage is presented here; technology projections are for the short term, less than 5 years. A computer simulation is developed to examine overall vehicle design. Vehicle characteristics, fuel cell polarization curves, and a Taiwanese urban driving cycle are specified as inputs. Transient power requirements reach 5.9 kW due to rapid acceleration, suggesting a large fuel cell. However, average power is only 600 W: a hybrid vehicle with a smaller fuel cell and peaking batteries could also handle the load. Fuel economies are greater than 500 mpge at steady-state driving. Results show that hybrid vehicles do not significantly improve mileage, but would drastically reduce the size of fuel cell needed. System size is approximately the same as present electric scooters, at 43 l and 61 kg for the fuel cell, hydrogen storage, and electric motor/controller, for a total scooter weight of about 130 kg.

Keywords: Scooter; Fuel cell vehicles; System modeling

1. Introduction

A conceptual design for a fuel cell scooter replacement that matches today's gasoline scooters is devised; a computer model is implemented to determine performance in comparison with published results. The fuel cell scooter represents a small but growing area of interest. A good example of previous work in a closely related area is a 1997 Princeton University thesis by Colella [1], which concerns the modeling and actual construction of a fuel-cell assisted bicycle with reference to Thailand conditions. A useful counterpoint to this modeling work is LaVen's work on building and testing a prototype metal hydride-powered fuel cell scooter at the Desert Research Institute [2]. The purpose of this study is to design and simulate a fuel cell replacement for today's scooter in Asia. Scooters are defined as small two-wheeled vehicles that can carry one or two people. They are between motorcycles and bicycles in power, but unlike both in that they are ridden in a seated position with feet forward on a platform. The size focused on here is the midrange 5 kW scooter, comparable to 50 cc internal-combustion-engined scooters.

The performance specifications are converted to power requirements using a model of road performance, scooter physical parameters, and the Taipei Motorcycle Driving Cycle. Using the performance requirements calculated from these variables, a fuel cell and a metal hydride storage system are configured. The weight and performances of these components are, in turn, returned to the model to produce the final performance of the scooter in terms of fuel consumption and parasitic power losses. A final section describes how a hybrid scooter with a peaking power battery would allow a smaller fuel cell to be used, reducing capital cost.

First, the possible market and the performance requirements are detailed, in order to set a target for a technical discussion.

With 10 million scooters and a progressive policy towards electric scooters, Taiwan is an excellent case study [3]. Especially high-polluting two-stroke vehicles made up

* Fax: +1-609-258-3661; e-mail: brucelin@alumni.princeton.edu

0378-7753/00/$ - see front matter
PII: S0378-7753(99)00480-2

Table 1
Fuel cell scooter performance requirements
The slope climbing, acceleration, and maximum speed requirements are based on a Taiwan electric scooter proposal, which in turn was based on surveys of scooter users; the maximum power is comparable to 50 cc i.c.l. scooters [9].

Specification	Fuel cell scooter
Max motor power output	4–6 kW
Range before refueling	200 km at 30 km/h
Fuel efficiency	>100 mpge
Acceleration	0–30 km/h in less than 5 s
Speed on 15° slope	10 km/h
Speed on 12° slope	18 km/h
Maximum speed	60 km/h
Curb weight	<130 kg

40% of all vehicles in Taipei in 1996; this is the impetus for change [4]. Fuel injection, catalytic oxidation of exhaust gases, and a switch to four-stroke engines have all been proposed as solutions to this highly visible problem; all of the options have been estimated to add approximately 50–100% to the approximately US$150 manufacturing cost of the two-stroke engine, with reductions in hydrocarbon emissions of 40–80% and 40–90% for carbon monoxide [5]. However, the Taiwan government has mandated a move towards further reductions in the form of zero-emission scooters [6,7].

The first battery-powered electric scooters have failed to capture significant market share because they are inconvenient to recharge, and because they simply do not match the power and range of existing alternatives. Electric scooters are presently at the low end of scooter engine power at 3 kW. Urban driving in Asia often requires bursts of acceleration to dodge between larger vehicles in congested traffic and this calls for high power. Electric scooters will never replace a third of two-stroke scooters if their competitors have four times the range, with quicker refueling. Additionally, mass is an important consideration also: a curb weight, the weight of vehicle without passengers or cargo, of approximately 130 kg approaches the limits of manageability for parking and unpowered handling [8]. In order to succeed, the technology must be able to match the performance of at least today's low-end gasoline scooters, as Table 1 illustrates.

2. Initial modeling results

In this section, the computer model and its important inputs are described; initial results, dependent only on the physical characteristics of the scooter and not power system characteristics, are laid out. Then, the Taipei Motorcycle Driving Cycle is used to calculate maximum power under the irregular velocities of typical urban driving conditions.

2.1. Model

The computer model design ''launch14'' calculates the instantaneous power required from a scooter's engine as it travels through various driving patterns. The model is based on a standard road load model. First, the mechanical power P_{wheels}, demanded at the wheels by the motion of the vehicle is:

$$P_{\text{wheels}} = (mav) + (mgv\sin\theta) + (mgvC_{\text{RR}}\cos\theta) + \left(1/2\ \rho_{\text{air}} C_{\text{D}} A_{\text{F}} v^3\right) \quad (1)$$

where m = total mass of vehicle, people, and cargo; θ = angle of slope; a = instantaneous acceleration of vehicle; v = instantaneous velocity of vehicle; C_{RR} = coefficient of type rolling resistance; ρ_{air} = density of air, approximately 1.23 kg m^{-3}; C_{D} = drag coefficient; and A_{F} = frontal area.

Regenerative braking is possible when acceleration is negative and when the first negative term exceeds the other terms. Parameters for a typical scooter are listed in Table 2 with data for other vehicles for comparison. Next, the inefficiencies in the system are applied to determine how much power must be developed by the power source:

$$P_{\text{output}} = (P_{\text{wheels}})/\eta_{\text{drivetrain}} + P_{\text{auxiliary}} + P_{\text{parasitics}} \quad (2)$$

$P_{\text{auxiliary}}$ = power needed by auxiliary systems — headlights, signal lights, dashboard, etc.; $\eta_{\text{drivetrain}}$ = efficiency of the electric motor and controller subsystem — 77%; $P_{\text{parasitics}}$ = parasitic power needed by fuel cell system — blowers, fans, etc.

The parasitic and auxiliary powers are electric power requirements so they do not suffer the 77% efficiency loss. A more sophisticated model would not use a single value of $\eta_{\text{drivetrain}}$, but rather employ an efficiency map to determine electric motor efficiency as a function of wheel speed and torque. The typical variation over the map for electric motors of the size required here is of the order of 5%, so this expedient was not adapted here.

Table 2
Typical modeling parameters collected from the literature [10–17]

Vehicle	C_{RR}	C_{D}	A_{F} (m^2)	Curb weight (kg)	Auxiliary power (W)
Electric scooter	0.014	0.9	0.6	130	60
Roadster bicycle	0.008	1.2	0.5	10	0
Motorcycle	Unknown	0.6	0.8	300	Unknown
Ford AIV Sable	0.0092	0.33	2.13	1291	500
PNGV automobile	0.007	0.20	2.0	920	400

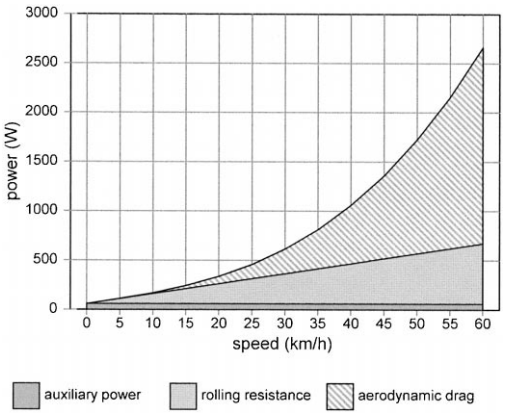

Fig. 1. Cruising power required at various speeds.

The total curb weight was set at 130 kg, which was 30 kg more than a Taiwan prototype ZES-2000 but equal to that of Honda's CUV-ES electric scooter. The driver weight was 75 kg. Auxiliary power was an average of 60 W.

Power requirements are shown for (i) a scooter travelling at constant velocity on various slopes (Fig. 1), and (ii) a scooter traveling with constant velocity at various speeds (Fig. 2). The total power plotted is the electric output from the power source including auxiliary power, but not subsystem parasitic loads (blowers, pumps, etc.) which are calculated later.

According to the model, continuous hill climbing as set out in the requirements (10 km/h at 15°, 18 km/h at 12°) require 2050 W and 3020 W from the electric power source, respectively. Cruising at 30 km/h requires 615 W. Cruising at 60 km/h requires 2600 W. Maximum continuous power output, under the requirements, is thus 3020 W net.

A comparison with published power requirements (Fig. 3) show good correlation with performance requirements quoted by T.C. Pong, an electric scooter designer; data was measured from road tests of a Sun Com scooter by Arne LaVen of the Desert Research Institute and published ITRI ZES-2000 results [18–20].

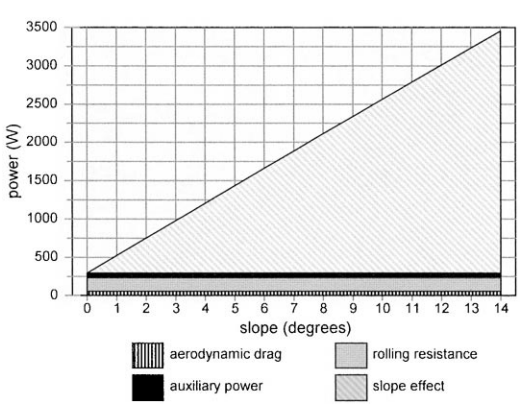

Fig. 2. Power required to climb various slopes at 18 km/h.

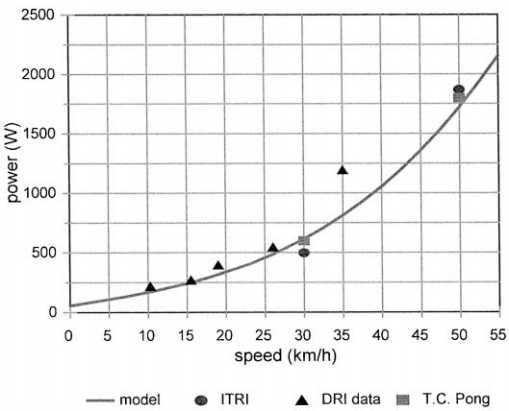

Fig. 3. Validation of physical model. Scooter properties for the other vehicles were not necessarily the same as used here. The results are for P_{output} *without* parasitic power, although they do include auxiliary power load and drivetrain efficiencies.

2.2. Driving cycle

Steady-state modeling is not sufficient to characterize the stop–go travelling common to urban driving, or acceleration requirements. The Taipei Motorcycle Driving Cycle (TMDC) is used to calculate maximum power and average power for urban driving. Developed by researchers at the Institute of Traffic and Transportation at Taiwan's National Chiao Tong University, the TMDC (Fig. 4) is an actual velocity trace obtained by researchers who followed target vehicles on an instrumented chase vehicle [21]. Due to errors in the original data and very high accelerations, the TMDC was smoothed with a low-pass filter to reduce the maximum power to approximately 5.0 kW to match the predefined performance requirements and to match scooters with the 50 cc two-stroke engines targeted here. The low-pass filter was a transfer function defined to have a DC gain of 1, in order not to change the average velocity profile; it had a time constant of 3.1 s.

Running the model with the TMDC shows the power profile of Fig. 5. The results are summarized in Table 3 and compared with steady-speed cruising.

The model shows that acceleration power demands the greatest peaks in the cycle, and also accounts for most of the energy in the cycle, not including braking energy recovered from negative acceleration. Rolling resistance accounts for somewhat less energy, and aerodynamic drag even less. The 60 W of auxiliary power is at most 10% of the average power. Only small improvements are likely to come from improved aerodynamics or rolling resistance, and the acceleration profile is inherent in the way the scooter is driven; for this component, energy use can only be reduced by reducing mass. One important ramification of the high acceleration and deceleration is that a significant amount of energy can, theoretically, be recovered by

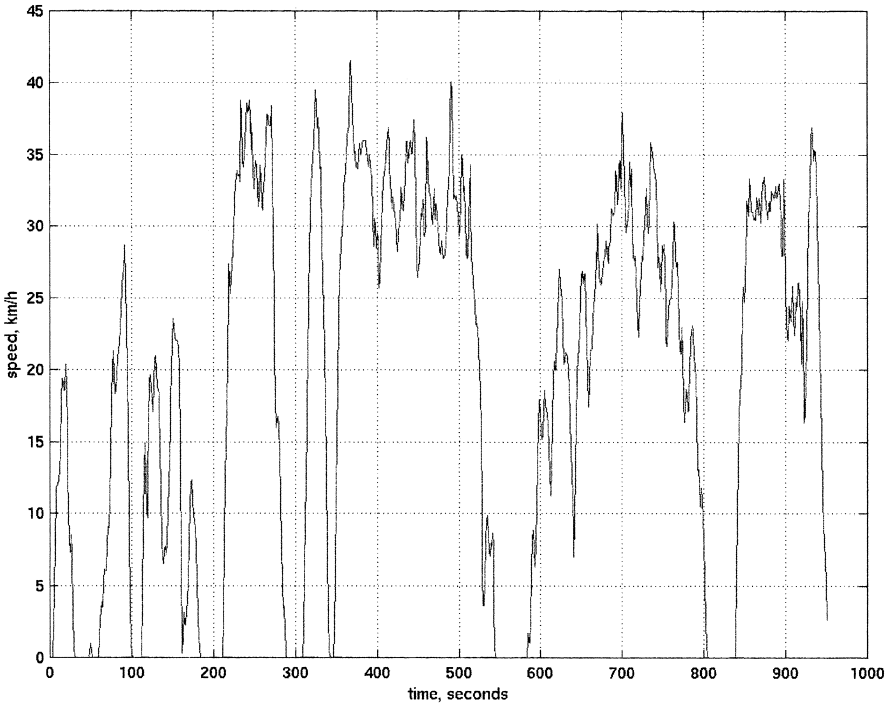

Fig. 4. Smoothed TMDC.

regenerative braking; the energy dissipated in braking is an average of 122 W (20% of the 566 W engine output).

Another result of the irregular velocity pattern and low average speed is that the average power requirement is

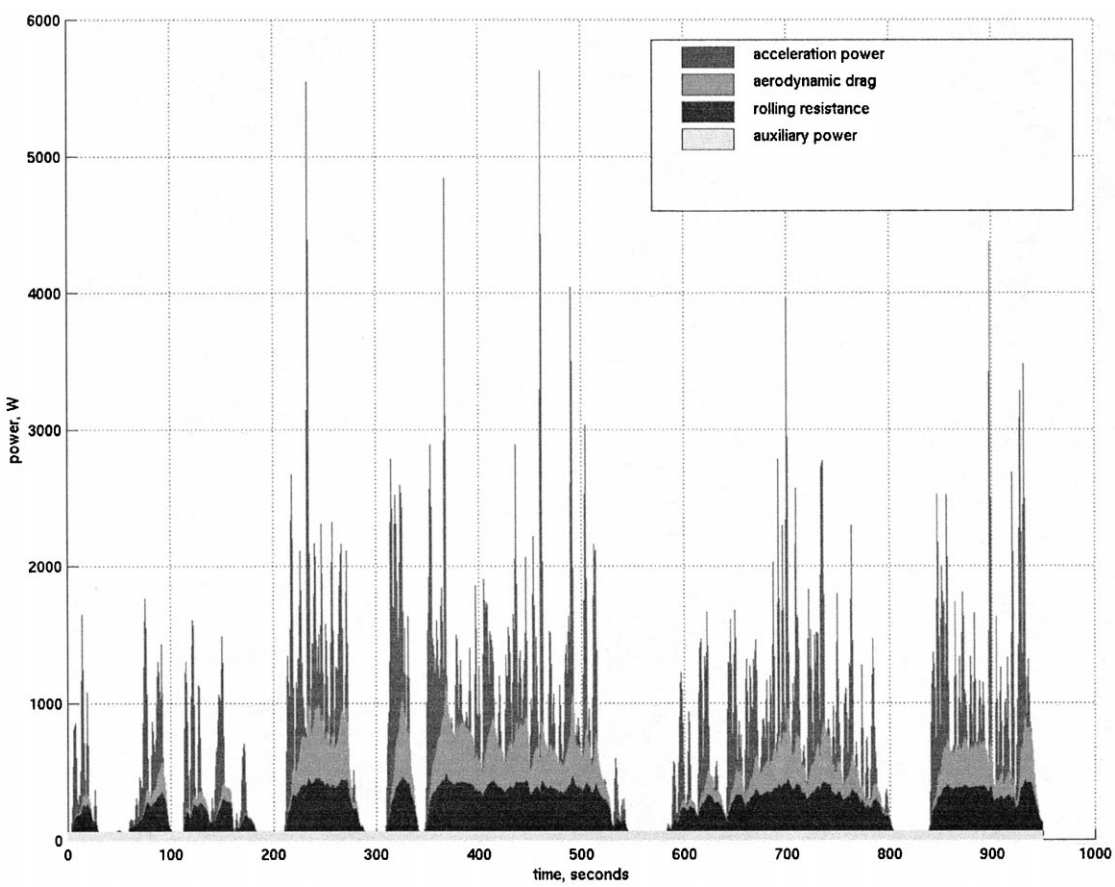

Fig. 5. Power required in TMDC.

Table 3
Model power requirements for driving cycle and for steady state driving

	TMDC	30 km/h
Total time	950 s	–
Average speed	19.3 km/h	30 km/h
Maximum speed	46 km/h	30 km/h
Maximum acceleration	6.4 km/h/s	–
Maximum deceleration	−8.6 km/h/s	–
Maximum net power from engine (includes drivetrain)	5.6 kW	615 W
Average power from engine (no parasitics; includes drivetrain)	566 W	615 W
Average acceleration power (positive only)	215 W	–
Average rolling resistance power	151 W	305 W
Average aerodynamic drag power	117 W	250 W
Mileage in terms of electric output	35.5 km/kWh	48.8 km/kWh
Total energy storage for 200 km	5.6 kWh output	4.1 kWh output

only one tenth of the maximum power. The extreme variability in the power demands suggests that hybridization would be useful, with a battery providing surges of extra power during bursts of acceleration and also the capability to store braking energy.

Steady-state driving actually requires more power, as Table 3 shows, although efficiency is higher. A complete analysis of fuel economy, however, requires a polarization curve of efficiency versus net power, and an understanding of the parasitic power. Note that a total of 4.1 kWh output is needed to store enough electricity for 200 km of range at 30 km/h, about three times the amount stored by today's scooter batteries.

3. Power system

This section calculates the characteristics required of a fuel cell power system, based on the assumption that present state-of-the-art performance can be implemented in stacks for commercial scooters in the next few years. The operating point and maximum current density of the stack are defined based on a polarization curve. Metal hydride storage performance is described, so that both fuel cell and storage system can be integrated with the model to provide final performance parameters.

3.1. Fuel cell stack

A maximum gross fuel cell power of 5.9 kW is calculated from the maximum TMDC requirement of 5.6 kW net power plus 300 W for parasitic power losses, vide infra. The polarization curve of Fig. 6 is a published result for laboratory-bench atmospheric-pressure cells; these are extrapolated to predict future stack performance.

Maximum power (5.9 kW) is designed to occur just before the peak at 1000 mA cm^{-2}. Here, power density is 614 mW cm^{-2} and thus 9.6×10^3 cm^2 of active area are needed. The average TMDC power demand is 566 W; later modeling shows that the final result including parasitic power, after iterative calculation, is 674 W and at this level the power density is 70 mW cm^{-2}. The system is designed to run at a motor-standard 48 V at this point, requiring 56 cells of 170 cm^2 each. Dc-to-dc conversion is required and losses are included in a 77% drivetrain efficiency. Three different situations are summarized in Table 4. On average, current density is extremely low, corresponding to high efficiencies. Occasional excursions to high currents are required for maximum acceleration.

3.2. Subsystems and parasitic losses

The gas supply, water, and cooling subsystems are designed to be as basic as possible. They are used to calculate parasitic power for the model.

Pure hydrogen fuel is supplied closed-ended in the design proposed here, so that there is no anode outlet. Effective utilization is slightly less than 100% due to the need for occasional purging, although here this loss is assumed to be negligible. The blower power required on the air side is:

$$\dot{W} = \frac{\Delta P \dot{V}}{\eta} \tag{3}$$

where η is the blower efficiency. With a 50% blower efficiency, estimated 2 psi air drop within the cell, and a maximum 15.6 cfm of air flow as required by 2.5× stoichiometry, this represents a maximum theoretical power consumption of 200 W. The blower power was modelled in the simulation as a linear 50–250 W load from 0 to 6 kW of output. This is a conservative calculation based on comparison with a reported parasitic power requirement of 105 W for a 24 VDC Ametek blower at 1.3 psi for a 4-kW nominal power fuel cell [23].

Humidification is assumed to be implemented internally whilst operating at 50°. The lower temperature reduces evaporation, but incurs the cost of more difficult cooling

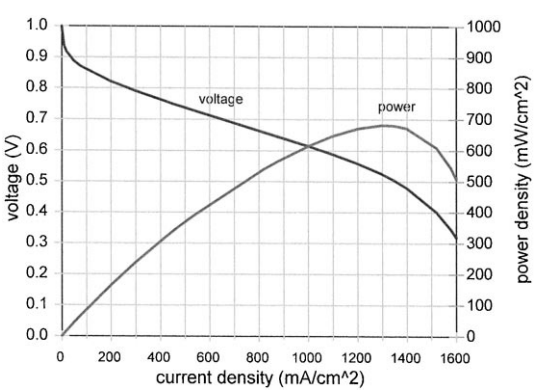

Fig. 6. Polarization curve. Data from Barbir is for a single cell running on hydrogen/air at atmospheric pressure, with a Gore MEA and operating temperature of 60°C. Air-side stoichiometry is 2.5 [22].

Table 4
Fuel cell design parameters

	Maximum power	Hill climbing continuous power	Average TMDC power
Power with parasitic load	5.9 kW	3.2 kW	674 W
Current density	1000 mA cm^{-2}	448 mA cm^{-2}	81 mA cm^{-2}
Stack current	172 A	76 A	14 A
Cell voltage	0.61 V	0.75 V	0.87 V
Power density	614 mW cm^{-2}	336 mW cm^{-2}	71 mW cm^{-2}
Efficiency	41%	51%	59%

due to a smaller temperature difference with the environment.

Cooling is the final subsystem dealt with here. Heat is generated by the fuel cell and two removal mechanisms are analyzed: active cooling with a liquid coolant loop discharging heat through a radiator to the environment, and heat removal from the desorption of hydrogen from a metal hydride storage cylinder. The pump circulating the coolant, and a fan blowing air over the radiator both require parasitic power; a backup system such as a resistance heater might be necessary for startup and active control of the metal hydride temperature, but is not included here.

Maximum heat production is 8.4 kW. (In comparison, a 20% efficient 5-kW internal combustion scooter engine outputs 20 kW of waste heat; the difference is that this load is produced at high temperatures and, thus, is easily rejected to the environs by air blowing over cooling fins.) The TiFe metal hydride system consumes 28 kJ of heat per mole of hydrogen desorbed. This is 1.4 kW (16.7%) of the waste heat at maximum power; the percentage increases to a maximum of 30.2% as the fuel cell is throttled back to lower powers, because the number of moles of hydrogen per unit of heat output increases due to the greater efficiency.

A maximum fuel cell temperature of 65°C is defined to avoid drying out the membrane, and the worst-case ambient temperature is set to 40°C ($\Delta T = 25$°C).

Over the TMDC, the average heat generated is 742 W, only 393 W after hydride heat absorption is included, and peaks in heat generation are very brief in duration, so continuous heat generation is of the greatest concern. At 3200 W continuous gross output, the rate of waste heat generation is 3.1 kW. The metal hydride eliminates 20% at this power level, leaving 100 W/K that must be dissipated for the fuel cell; an extra margin of 10 W/K was added for a design specification of 110 W/K. At this level, the parasitic power loads are 25 W for the coolant pump and 14 W for the radiator fan, based on radiator manufacturer data, plus the blower power of 50 W, at no load, to 250 W at maximum output 5.9 kW gross) [24]. The power is calculated as if the pump and fan were continuous, for a total parasitic load of 89–289 W over the output range of the fuel cell.

The parasitic power assumed is more conservative than that given in a study published by the Schatz Energy Research Center [25] (Fig. 7). The Schatz graph represents the parasitic power requirements for a nominal 4 kW vehicle (golf cart) fuel cell stack operating at atmospheric pressure. The system operates at approximately 40°C, and the air flow rate at 1.74 kW is 4.5 cfm, which is approximately 60% higher at the same power than the system presented here.

3.3. Fuel storage

Direct hydrogen storage is selected to avoid the need for a bulky and expensive reformer on board the scooter; reforming requires additional equipment which comes at a premium on a small vehicle. Notwithstanding, it should be noted that recent developments in efficient reforming in microchannels with high specific surface area could change this situation in the future [26]. The hydrogen is stored by adsorption in to metal alloys. Metal hydrides were used in some demonstration fuel cell vehicles but due to their weight and expense, presently US$30/kg of hydride alloy, are not being considered for the first wave of fuel cell vehicles. Although metal hydrides suffer from the problems of high alloy cost, sensitivity to gaseous impurities, and low gravimetric hydrogen density, they have excellent volumetric storage density together with an inherent advantage of being endothermic when releasing hydrogen, thus reducing the risk of fire. In addition, the hydrogen is kept at a relatively low pressure of 1–10 atm within the

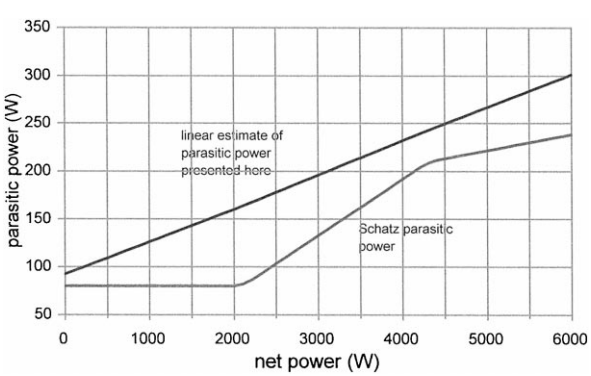

Fig. 7. Parasitics as a function of power.

Table 5
Theoretical performance of low-temperature metal hydride
Storage system includes container and heat exchange equipment, estimated by Browning et al. as an extra 100% and by Le of NASA at an extra 50% [30,31]. The latter assumption is used here.

	$FeTiH_{1.9}$
H_2 storage by weight	1.75%
Density of metal hydride	5.47 g cm^{-3}
H_2 storage by volume	101 g/l
Heat of desorption ΔH (kJ mol H_2^{-1})	−28.0
Dissociation temperature	50°C
Desorption pressure at given temperature	10 atm
Hydrogen stored for 200 km	250 g
Total storage system mass	21.4 kg
Total storage system volume	3.7 l
Effective storage by weight	1.2%

metal hydride containment vessel rather than the 250 atm of compressed gas cylinders, so the rate of hydrogen leakage is lessened and the risks of explosion in the case of collisions reduced. For a more detailed comparison of the various hydrogen storage options, refer to previous work [27]. The data in Table 5 on the hydride storage system were based on Browning et al. [28] and a DTI report on hydrogen storage [29].

For comparison, a gasoline tank in a scooter is about 5 l, contains approximately 3.7 kg of gasoline, and allows a range of 240 km at 30 km/h, while the battery used in the ZES 2000 scooter is 3.7 l and weighs 44 kg, but only provides 65 km of range at 30 km/h. An aluminum-carbon compressed gas cylinder at 3600 psi would occupy 31.5 l and 11 kg for the same 250 g of storage [32].

4. Modelling results

4.1. System performance

The complete model takes the vehicle physical model and integrates the efficiency of the motor/controller subsystem, parasitic power demands, and the fuel cell polarization curve to determine overall efficiency: this represents the amount of hydrogen consumed for a given travel distance under both the Taipei Motorcycle Driving Cycle and steady state 30 km/h driving conditions. The overall performance is used to identify the sizing of subcomponents like the fuel storage supply and, thus, to determine the overall system weight and size. The same basic model, minus parasitic power, is used to obtain performance for a battery-powered option undergoing the same driving. The results are presented in Table 6. The battery energies are given in terms of total energy *output*; actual performances are lower due to charging and discharging inefficiencies.

Extremely high mileages are realized, over three times today's gasoline scooters for the TMDC case, although it should be noted that the comparison is not exact because there is an efficiency loss when fossil fuels are reformed to hydrogen. Efficiencies are higher for 30 km/h cruising due to the lack of high-current excursions.

4.2. Size and weight of power system

Fuel cell size and weight were calculated based on a DTI study of fuel cell stack construction for automobiles [33]. One cooling cell is assumed for every two active cells, but with a shorter stack than the 420-cell versions used in that report. The results are listed in Table 7 with the auxiliary components required.

The fuel cell stack performance is 780 W/kg and 760 W/l, slightly less than 1996 Ballard stacks at 1 kW/l. With auxiliaries, the densities are 240 W/kg and 200 W/l. The stack proper takes up 27% of the mass and 26% of the volume. In comparison, the PNGV Technical Roadmap fuel cell system requirements are 0.4 kW/kg and 0.4 kW/l [34], while the overall fuel cell system weight of the 4-kW Schatz Energy Research Center Personal Utility Vehicle was 90 kg. Stack volume was 10 in. × 11 in. × 21 in., or 39 l [35]. With the greater room of a golf cart, engineering for minimum volume is not so critical, but this information does warn that reduced size and weight have not yet been demonstrated at the 5-kW size.

The TiFe metal hydride storage cannister for 250 g of hydrogen is 21 kg and 4 l, for a total power system weight of 61 kg and volume of 43 l. This corresponds to the weight of the existing ZES drive system (battery + motor + controller), suggesting that the 130 kg target curb weight is reasonable. In addition, the extra performance provided by the 5.6 kW fuel cell system partially compensates for the high mass. Figs. 8 and 9 show the distribution of size and weight for the various subsystems.

In sum, the fuel cell vehicle offers more than three times the range of the ZES-2000, with roughly the same weight of drive system. The fuel cell systems does require 18 to 36 additional liters of storage space over that of the

Table 6
System performance under TMDC and at cruising speed

	TMDC	30 km/h cruise
Maximum power from fuel cell (includes drivetrain and parasitics)	5.91 kW	725 W
Average fuel cell output power	674 W	725 W
Overall efficiency	46.7%	58.5%
Fuel economy relative to hydrogen	0.527 km/g H_2	0.807 km/g
Equivalent ''on-vehicle'' fuel economy	344 mpge	522 mpge
Hydrogen storage for 200 km range	380 g	248 g
Average output power without parasitics (battery powered scooter)	566 W	614 W
Fuel economy of equivalent battery powered scooter	35.5 km/kWh	48.8 km/kWh
Battery energy storage for 200 km range	6.5 kWh	4.1 kWh

Table 7
Size and weight summary

	Brand	Model	Dimensions (in cm)	Size	Weight (kg)
Fuel cell stack	–	–	–	7.8 l	7.6
Starter battery	Yuasa	GRT YT4L-BS	11 × 7 × 9	0.7 l	1.3
Coolant pump	generic	–	8 × 12 × 12	1.2 l	1.0
Radiator with fan	Lytron	M14-120		15.2 l	8.9
Blower	Ametek	116638-08	15 diameter × 17 length	2.9 l	2.7
Plumbing, wiring, etc.	generic	–	–	2.0 l	3.0
coolant water	–	–	–	–	0.64
Total stack with auxiliaries	–	–	–	29.8 l	24.6

ZES-2000. There is a helmet storage chamber in the design that could be commandeered for additional fuel storage; this is approximately 10–15 l of space. The scooter body would have to be redesigned to make more room available, or the off-the-shelf radiator would have to be reduced in size. Note that present electric scooters already use redesigned large-capacity bodies, so additional volume increases may prove difficult.

5. Hybrid design

A peaking power battery allows a smaller fuel cell to be used, and also enable energy to be saved through regenerative braking. The major drawback is that hybrid systems require more complex controls and power conditioning systems. Two options are presented here: a hybrid that meets all the performance requirements, and a scaled-down version of only 1 kW that cannot sustain continuous hill climbing for as long. Performances are calculated as before, size and weights of the subsystems are estimated, and finally, presently available fuel cell stacks are compared.

5.1. Hybrid description

Two hybrids were specified, both capable of sustaining maximum power for at least 10 s. The first had to maintain the same performance as the pure fuel cell scooter, including sustaining 3.2 kW gross power for indefinite hill climbing. The second case targets the short term where fuel cells are extremely expensive and size must be minimized at all costs; it uses a 1.1 kW (gross) fuel cell, with a large battery for the remaining 4.6 kW. This scooter would not be capable of sustaining the hill climbing requirements; the specified performances could only be achieved for under 3 min until the batteries drain down to their 20% limit and the continuously sustainable hill climbing speeds are lower than the requirements.

Cooling load is significant in hybrid vehicle design as well as in the original pure fuel cell design; again, the critical situation is the hill climbing, requiring 3.2 kW of continuous output. In the 5.9-kW full-sized fuel cell, continuous operation at 3.2 kW gross output takes place at 51% efficiency, and heat production is consequently low. A 3.2-kW maximum power fuel cell, however, is only at 43% efficiency when it is continuously operated at the same power, producing more heat. The greater heat also necessitates higher pump and fan loads for the radiator, meaning greater parasitic loads. The 1.1-kW system was easier to solve because the output was simply capped at 1.0 kW of net output.

The different hybrid requirements are summarized in Table 8.

Note that a 35-cm^2 cell is extremely small, and while not the most efficient cell size, avoids having to completely redesign the system. A more realistic approach would be to use larger and fewer cells, at the cost of additional dc-to-dc conversion losses, which unfortunately could not be investigated given the time constraints here.

The peaking power source is modelled upon the Bolder Technologies advanced lead-acid battery, which offers high power density at relatively low cost. The low energy density is not a significant factor in the brief-peaking

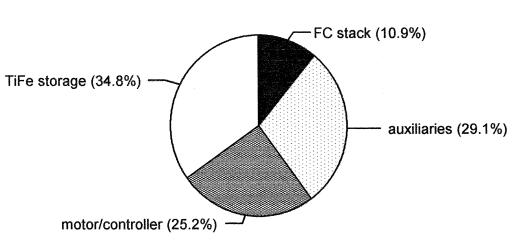

Fig. 8. Weights of subsystems. The total drive system weight is 61 kg.

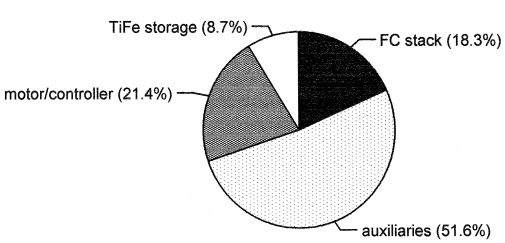

Fig. 9. Volumes of subsystems. Total 43 l.

Table 8
Hybrid fuel cell stack designs

	Pure FC	Hybrid 1	Hybrid 2
Maximum gross power	5.9 kW	3.2 kW	1.1 kW
Stack current at maximum power	172 A	89 A	31 A
Efficiency at maximum current density	41.2%	43.2%	43.6%
Total active area needed	9600 cm^2	5600 cm^2	2000 cm^2
Active area per cell	170 cm^2	100 cm^2	35 cm^2
Maximum heat generation (after metal hydride cooling)	7.0 kW	3.5 kW	1.2 kW
Cooling factor needed at maximum power ($\Delta T = 25$°C)	280 W/K	140 W/K	50 W/K
Cooling factor at continuous 3020 W	110 W/K	140 W/K	50 W/K (at 1 kW)
Cooling fan power requirement at continuous 3020 W	14 W	28 W	4 W (at 1 kW)
Coolant pump power requirement at continuous 3020 W	25 W	38 W	21 W (at 1 kW)
Maximum net fuel cell power	5.9 kW	3.0 kW	1.0 kW
Battery power needed	–	2.6 kW	4.6 kW

pattern of Taiwan driving. The battery modelled here has a density of 1 kg/l, power density of 840 W/kg for a 40-s discharge and an energy density of 17 Wh/kg; its performance is slightly lower than the 100 kW version used in the Chrysler Intrepid ESX hybrid [36–38]. Battery efficiency was based on a semi-empirical model developed by the Center for Energy and Environmental Studies at Princeton University [39]. In this model, discharge and charge efficiencies are of the order of 90–95%.

For regenerative braking, 30% of the energy is simply unavailable, as reported by an NREL paper, due to frictional and other losses [40]. For the generation of electricity from this kinetic energy by driving the electric motor in reverse, a 77% efficiency is assumed. Power is divided between fuel cell and battery according to the following rules.

(1) The state of charge of the battery must stay between 80% and 20% to avoid permanent battery damage.
(2) Initial state of charge is 50%.
(3) The battery makes up the difference whenever the fuel cell maximum power is not enough for the driving cycle power plus auxiliary and parasitic loads.
(4) Regenerating always recharges the battery as long as the maximum charging current is not exceeded, up to 80% SOC.
(5) The battery is charged up from the fuel cell at a specified rate whenever (i) the state of charge dips below 55% and (ii) power demand at that instant is less than 400 W. The charging rate is equal to 400 W minus the instantaneous power demand from the wheels, auxiliaries, and parasitics.

5.2. Hybrid simulation results

The results in Table 9 show that steady-state driving shows decreasing efficiency as smaller fuel cells are used, while urban driving exhibits the opposite trend. The 3.2-kW size suffers from higher parasitic losses due to its more demanding heat generation.

Efficiency decreased as the fuel cell size decreased, because the smaller fuel cells were operating closer to their maximum output. The driving cycle results in Table 10 are more interesting because deceleration created the possibility of regenerative braking.

The 1.1-kW fuel cell provides 100 W less average power than the 5.9 kW fuel cell, because the 86 W (average) that is recovered from regenerative braking can supplement the peaks. Again, the fuel cell was operating more frequently near its lowest efficiency (maximum power) and the result is a net fuel economy that is virtually the same as the pure fuel cell. However, this design reduces the size of the fuel cell stack by a factor of more than 5, which is important for the short term cost.

For the 3.2-kW fuel cell in both cases, fuel economy decreases significantly with hybridization. There are three

Table 9
Hybrid performance at 30 km/h

Parameters	5.9 kW pure FC	3.2 kW hybrid	1.1 kW hybrid
Fuel cell conversion efficiency	58.5%	56.4%	50.0%
Average fuel cell output power	725 W	751 W	710 W
Fuel economy in terms of hydrogen	0.807 km/g	0.751 km/g	0.703 km/g
''on-vehicle'' fuel economy (change from pure FC)	522 mpge (0)	486 mpge (−4%)	455 mpge (−15%)
Hydrogen for 200 km	248 g	266 g	284 g

Table 10
Hybrid performance under TMDC

Parameter	5.9 kW pure FC	3.2 kW hybrid	1.1 kW hybrid
Fuel cell maximum power	5.91 kW	3.24 kW	1.11 kW
Battery maximum power needed	–	2.61 kW	4.63 kW
Average total power output, battery + fuel cell	674 W	709 W	726 W
Average fuel cell power	674 W	698 W	577 W
''on-vehicle'' fuel economy (change from pure FC)	344 (0)	316 (−8.2%)	343 (−0.3%)
Conversion efficiency	56%	53%	47%
Average power regenerated	–	65 W	86 W
Braking energy recovered as a fraction of theoretical maximum braking losses	–	51%	68%

reasons: (i) the cooling system parasitic load is larger, (ii) the fuel cell is operating more frequently near its maximum load, and (iii) the battery is rarely used to output energy. Due to the lower fuel economy at 30 km/h, slightly more metal hydride is needed: 266 g for 200 km.

Battery energy does not return to initial levels over the driving cycle for the 3.2 kW hybrid — in fact, there is a net gain from regeneration of 58.3 kJ, or an average of 60 W over the 950-s cycle. This is a not insignificant amount of surplus energy that could be used to improve fuel economy, if a more sophisticated battery policy that intelligently predicted power usage could be used.

The same DTI model used previously was repeated to calculate fuel cell stack sizes and weights for the hybrids; other components were added to find total drive system mass and volume (Table 11). Peaking power batteries do not significantly reduce the mass and volume of the total fuel cell system, because the auxiliary cooling and fluid management systems require a certain minimum space and mass which does not decrease rapidly with size. Furthermore, hydride mass increases slightly with decreasing fuel cell size due to decreasing 30 km/h efficiency. The 1.1 kW hybrid does have much smaller volume due to the smaller radiator. On the other hand, certain other factors decrease almost linearly with fuel cell size, foremost among them membrane area and platinum cost. Significant cost reductions might be possible under such a system for the near future while fuel cells remain extremely expensive; unfortunately, these costs are not reflected in the price calculations above, which rely upon ultimate price estimates for mass-produced stacks.

5.3. Near-term possibilities

To obtain a rough comparison of these designs with what is available today, portable stacks from H-Power and Ballard were inserted into the 1 kW fuel cell design. A single PS-250 fuel cell unit commercially available from H Power produces 250 W net power, weighs 10.3 kg, and has a volume of 16 l [41]. The system is air-cooled, and with the correct geometry this could be viable for a scooter version. The existing design can actually output 330 W; to be conservative, retail units are sold derated to 250 W. Using three units to supply the 1.0 kW net output desired produces a power system weight of 31 kg and volume of 48 l. 1999 costs are of the order of US$6000 for a unit like the PS-250, with mass-production costs expected to drop to US$1000 [42]. For the three units required, then, the near-term cost would be on the order of US$18,000 and US$3,000 with mass production. On the other hand, Ballard Power Systems has developed a 1 kW (net power) stack that weighs 18 kg and has a volume of 33 l including all packaging [43]. These system sizes and weights are summarized in Table 12. In the short term, an unoptimized

Table 11
Component breakdown for hybrid scooter power systems

Component	3.2 kW		1.1 kW	
	Weight (kg)	Volume (l)	Weight (kg)	Volume (l)
Fuel cell stack	5.4	5.3	4.1	3.2
Auxiliaries	15.6	21.3	10.5	8.4
Peaking power battery	3.1	3.0	5.6	5.4
TOTAL STACK WITH AUXILIARIES	25.1	29.6	20.1	17.0
Motor and controller	15.5	9.1	15.5	9.1
Hydride for 200 km range	22.8 (266 g H_2)	4.0	24.3 (285 g H_2)	4.3
Total drive system	63	43	60	30

Table 12
Near-term 1-kW fuel cell hybrid designs
The fuel cell system size and weight exclude peaking power battery in all cases.

Parameter	As designed in this paper	Ballard stack	H-Power stack
Fuel cell system weight	14.6 kg	18 kg	31 kg
Fuel cell system volume	11.6 l	33 l	48 l
Fuel cell system power density, gravimetric	75 W/kg	61 W/kg	35 W/kg
Fuel cell system power density, volumetric	65 W/l	33 W/l	23 W/l

fuel cell hybrid based on Ballard performance figures would have a drive system at 63 kg and 51 l. This is 3 kg and 27 l more than the ZES-2000, which, although not as optimistic as present assumptions, is technically feasible in a scooter.

6. Conclusions

Existing and proposed battery-powered scooter designs have low performance and are not likely to displace combustion engined scooters until better range and power and recharging times arrive. However, in the time that batteries have to improve, fuel cells may offer an effective alternative. A fuel cell design was assumed here for the scooter that focused on simplicity on all fronts: pure hydrogen operation, atmospheric pressure, and low temperature. Metal hydride storage offers good synergy with the cooling system due to its endothermic hydrogen release, and greater safety than composite cylinders due to the lower pressures (1–10 atm). The results show that advanced fuel cell powered scooters could have more than three times the 100 mpg of existing gasoline-powered scooters, with zero tailpipe pollution, in a 130-kg package.

In addition, hybrid designs were examined in an effort to accelerate fuel cell scooter adoption by reducing the size of the fuel cell stack needed. Hybrid power systems with a combined peaking power battery offer significant reductions in cost because fuel cells are so expensive. Comparison with commercially available fuel cell technology reveals that the effective 1 kW scooter is possible today.

In the short term, phasing out two-strokes and speeding a transition to four-stroke engines offers rapid reductions in emissions. Nevertheless, a hydrogen fuel cell scooter is technically feasible, and offers additional air pollution reduction benefits over four-strokes, along with performance that batteries cannot yet match.

Acknowledgements

Thanks to Robert Socolow, Bob Williams, Joan Ogden, Tom Kreutz, and Srinivasan Supramaniam of Princeton University's Center for Energy and Environmental Studies, who all provided critical input into the original work. Research support came from the US Department of Energy, the Energy Foundation, and the Department of Mechanical and Aerospace Engineering. Finally, thanks to Whitney Colella (Oxford) and Arne LaVen (Desert Research Institute) whose work on similar topics was inspiring and whose comments were insightful.

References

[1] W. Colella, Electrically assisted fuel cell powered bicycle, B.S. Thesis, Princeton University Mechanical and Aerospace Engineering Department, Princeton Univ., 1997.
[2] A. LaVen, Energy and Environmental Engineering Center, Desert Research Institute, Personal communication, 1998.
[3] Directorate-General of Budget, Accounting and Statistics of Executive Yuan of the Republic of China, Monthly Bulletin of Statistics of the Republic of China, February 1999. Table K-5 Number of Registered Motor Vehicles http://www.dgbasey.gov.tw/dgbas03/english/bulletin/k5.htm.
[4] L. Underwood, Airborne Menace, Free China Review, September 1, 1996.
[5] B. Lin, Princeton University. Conceptual Design and Modeling of a Fuel Cell Scooter for Urban Asia, MSE Thesis, Princeton University Center for Energy and Environmental Studies, September 1999. Available at http://www.spinglass.net/scooters/
[6] C.S. Weaver, L.-M. Chan, Motorcycle Emission Standards and Emission Control Technology, Engine, Fuel, and Emissions Engineering, August 1994.
[7] Republic of China Environmental Protection Agency, Electric motorcycles targeted as key industry for development, Environmental Policy Monthly 1 (9) (1998) http://www.epa.gov.tw/english/Epm/issue9803.htm.
[8] P.H.J. Shu, W.-L. Chiang, B.-M. Lin, M.-C. Cheng, The Development of the Electric Propulsion System for the Zero Emission Scooter in Taiwan, Society of Automotive Engineers Paper No. 972107, 1997b.
[9] ibid.
[10] Highway Tire Committee, Society of Automotive Engineers, 1997.
[11] CALSTART web site, DARPA Consortia EV and Hybrid EV Technology Projects — (PNGV) Target Attributes, http://www.calstart.org/about/pngv/pngv-ta.html.
[12] Energy and Environment Analysis, Analysis of Fuel Economy Boundary for 2010 and Comparison to Prototypes, Prepared for Martin Marietta Energy Systems, Contract No. 11X-SB0824, November 1990, pp. 4–11.
[13] M. Ross, W. Wu, Fuel Economy Analysis for a Hybrid Concept Car Based on a Buffered Fuel-Engine Operating at a Single Point, SAE Paper 950958, presented at the SAE International Exposition, Detroit, MI, February 27–March 2, 1995.
[14] C.E. Thomas, B.D. James, F.D. Lomax, I.F. Kuhn, Jr., Integrated Analysis of Hydrogen Passenger Vehicle Transportation Pathways, draft final report, Directed Technologies for NREL, subcontract AXE-6-16685-01, March 1998.

[15] B.E. Bayer, Motorcycles, Chap. 10, in: W.-H. Hucho (Ed.), Aerodynamics of Road Vehicles, 4th edn.
[16] A. LaVen, Driving Cycle Analysis of the Sun Com™ Battery Electric Scooter, Energy and Environmental Engineering Center, Desert Research Institute, November 1998.
[17] W.-L. Chiang, Power Machinery Division Director, MIRL ITRI, personal communication, September 1998.
[18] T.-C. Pong, personal communication, October 1998.
[19] A. LaVen, 1998.
[20] C.-T. Liu, B.-M. Lin, J.-S. Pan, 1996.
[21] J.-J. Chen, personal communication, October 1997.
[22] F. Barbir, Operating Pressure and Efficiency of Automotive Fuel Cell Systems, Energy Partners, no date; 1997 or later.
[23] C.E. Chamberlin, Schatz Energy Research Center, personal communication, May 1999.
[24] Lytron web site. Lytron OEM Heat Exchangers (Radiators) Performance Curves. http://www.lytron.com/Catalog/oemperf.htm, June 1999.
[25] P.A. Lehman, C.E. Chamberlin, Design and Performance of SERC's Fuel Cell Powered Vehicle Fleet, Fuel Cell Seminar Abstracts, 1998, 714–717.
[26] Pacific Northwest National Laboratory web page. http://www.pnl.gov/microcats/fullmenu/compfuelproc.html.
[27] B. Lin, 1999.
[28] D. Browning, P. Jones, K. Packer, An investigation of hydrogen storage methods for fuel cell operation with man-portable equipment, J. Power Sources 65 (1997) 187–195.
[29] B.D. James, G.N. Baum, F.D. Lomax, C.E. Thomas, I.F. Kuhn, Jr., Comparison of Onboard Hydrogen Storage for Fuel Cell Vehicles, Task 4.2 Final Report, Directed Technologies, prepared for Ford Motor Company under Prime Contract DE-AC02-94CE50389 to the US DOE.
[30] D. Browning, P. Jones, K. Packer, 1997.
[31] M. Le, Johnson Space Center, NASA, personal communication, August 1998.
[32] B. Lin, 1999.
[33] F.D. Lomax, B.D. James, G.N. Baum, C.E. Thomas, Detailed Manufacturing Cost Estimates for Polymer Electrolyte Membrane (PEM) Fuel Cells for Light Duty Vehicles, Directed Technologies, prepared for The Ford Motor under Prime Contract No. DE-AC02-94CE50389 to the US DOE, Office of Transportation Technologies, August 1998.
[34] National Research Council, Review of the Research Program of the Partnership for a New Generation of Vehicles, Second Report, National Academy Press, Washington DC, 1996.
[35] S. Ornelas, Research Engineer, Schatz Energy Research Center, personal communication, February 1999.
[36] Bolder Technologies Rebel product data sheet, 1999.
[37] W. Woodley, Engineering Assemblies Corporation, personal communication, June 1999.
[38] Chrysler web site, ESX/Hybrid Technology Release Material, http://www.media.chrysler.com/wwwprkt/23a6.htm.
[39] T.G. Kreutz, M.M. Steinbugler, J.M. Ogden, S. Kartha, System Modeling of Fuel Cell Hybrid Electric Vehicles with Onboard Fuel Reformers, Center for Energy and Environmental Studies, Princeton Univ., unpublished paper, 1998.
[40] K. Wipke, M. Cuddy, D. Rausen, Using Systems Modeling to Facilitate the PNGV Technology Selection Process, Center for Transportation Technologies and Systems, National Renewable Energy Laboratory, presentation October 28, 1997 to 1997 Automotive Technology Development Customers' Coordination Meeting.
[41] R. Dubois, H. Power, personal communication, June 1999.
[42] A. Kaufman, H. Power, personal communication, May 1999.
[43] Ballard product data sheet, 1 kW fuel cell generator.